Materials Research
Express

PAPER • OPEN ACCESS

The proximity effect and critical field behavior of Re/Al bilayers

To cite this article: F N Womack *et al* 2025 *Mater. Res. Express* **12** 046001

IOP Publishing Mater. Res. Express 12 (2025) 046001 https://doi.org/10.1088/2053-1591/adbab6

Materials Research Express

PAPER

The proximity effect and critical field behavior of Re/Al bilayers

F N Womack[1], Á M Ortega[2], S K Karna[3], D Graf[4] and P W Adams[1]

[1] Department of Physics and Astronomy, Louisiana State University, Baton Rouge, LA 70803, United States of America
[2] Department of Physics, University of Puerto Rico, San Juan, PR 00925, United States of America
[3] Department of Physics, Prairie View A&M University, Prairie View, TX 77446, United States of America
[4] National High Magnetic Field Laboratory, Tallahassee, FL 32310, United States of America

E-mail: padams2@lsu.edu

Keywords: superconductivity, proximity effect, critical field

CrossMark

OPEN ACCESS

RECEIVED
7 August 2024

REVISED
14 February 2025

ACCEPTED FOR PUBLICATION
26 February 2025

PUBLISHED
11 April 2025

Abstract

We report the perpendicular critical field H_{c2} properties of disordered Re-Al bilayers via magneto-transport measurements. The bilayers consisted of a $d_{Re} = 3$ nm bottom layer of Re and an upper Al layer with thickness varying between $d_{Al} = 0 - 3$ nm. We find that in this range of Al thicknesses, the bilayer transition temperature T_c increases with increasing Al thickness, although their monolayer counterparts have $T_c^{Re} > T_c^{Al}$. Furthermore, H_{c2} of the bilayers has a local maximum at an Al coverage of 1.5 nm with a critical field that is 50% larger than that of the standalone 3 nm Re film. At higher Al thicknesses H_{c2} drops rapidly but remains more than an order of magnitude greater that that of comparable thickness standalone Al film. Our data show that a thin, disordered Re under-layer can dramatically increase the magnetic field tolerance of the Al over-layer. This would allow one to retain the desirable chemical and metallurgical properties of Al without sacrificing high field compatibility in quantum circuits, such as topological qubit devices and superinductor circuits.

1. Introduction

In this report we present upper critical field measurements of thin superconducting Re/Al bilayers. We consider the case where the bilayers are in intimate electrical contact and hence their superconducting properties can be described via the classic proximity effect [1, 2]. Historically, the proximity effect was first studied in a bilayer geometry [3] with one layer consisting of a robust superconductor such as Pb and the other a low T_c metal such as Al or perhaps a non-superconducting metal. By depositing a normal-metal film N on a superconducting film S one can induce superconductivity in N via the leakage of Cooper pairs from S to N. Conversely, the normal metal has a detrimental effect on the condensate in the S layer, and thereby lowers its transition temperature by an amount that depends upon the relative thickness of the two layers and quality of the coupling between the layers [4]. The present work is motivated, in part, by the recent discovery that thin, disordered, Re films exhibit extraordinarily high perpendicular critical fields [5, 6]. Indeed, the H_{c2} of films with thicknesses $3 - 6$ nm can be more than an order of magnitude larger than what is typical of elemental superconductors. In this light, the Re/Al bilayers system offers one the opportunity to study the proximity effect from the somewhat novel perspective of critical field behavior. Almost all previous studies of the classic proximity effect have been limited to its modulation of the transition temperatures and/or energy gap of bilayer components [1, 2]. Here we demonstrate that a thin, disordered layer of Re can enhance both the transition temperature and the perpendicular critical field of the Al component of the bilayer. This affords a relatively straightforward strategy for improving the field compatibility of the Al component of the bilayer [7–9]. In principle, bilayers with rather robust field compatibility could be used to replace the pure Al components of devices such as superinductor fluxonium qubits [10–13] and superconductor-semiconductor hybrid systems [14, 15]. In principle, this would allow one to retain the desirable chemical and metallurgical properties of Al without sacrificing high field compatibility.

2. Experimental methods

Rhenium-aluminum bilayer films were formed by e-beam deposition from Re and Al targets. The Re targets were produced by arc-melting 99.9% Re powder to form $3-5$ mm diameter buttons. The Al targets were made from clippings of 1 mm diameter 99.999% Al wire. The depositions were made onto fire-polished glass slides in a vacuum of $P < 3 \times 10^{-7}$ Torr and a rate of ~ 0.5Å/s. In order to minimize island formation and oxidation in the films, the substrates were held at 84 K during the deposition, thus the films were effectively quench-condensed onto the cryogenic substrates. The films and their corresponding contact pads were patterned by depositing through stencil masks placed in contact with the substrate. The contact pads were formed by first depositing 3 nm of Cr onto the film legs followed by 7 nm of Au. The Cr served to improve the adhesion of the gold pads. Electrical contact to the bilayers was made by soldering 1 mil Pt wires directly onto the contact pads using Wood's metal. This proved to be a much more reliable method of attaching leads than gluing the wires to the pads with silver paint.

All of the bilayer samples were formed by first depositing a 3 nm Re layer onto the glass substrate and then immediately depositing a Al layer directly onto the Re layer without breaking vacuum or warming the substrate. The samples used in this study had varying Al thicknesses up to $d_{\mathrm{Al}} = 4.0$ nm. Film thickness was determined via a quartz crystal thickness monitor located in the deposition chamber. Its accuracy was ± 0.2 nm. Magneto-transport measurements were made using a Quantum Design Physical Properties Measurement System having a maximum applied field of 9 T and a base temperature of 1.8 K. A standard 4-wire technique was used to probe the film resistivity. All of the transport data presented below is in terms of sheet resistance (resistance per square) as determined from the sample dimensions. The transport measurements utilized a probe current in the range 0.1μA to 4μA. Lower currents were used in the higher resistance samples. Care was taken to insure that the currents were sufficiently low to avoid self heating.

3. Theoretical background

Typically the critical field of a BCS superconductor is mediated by the orbital response of the conduction electrons to the applied field. However, if orbital response is suppressed, then the Zeeman splitting of the conduction electrons [16, 17] will limit the critical field. The Zeeman critical field can be an order of magnitude larger than its orbital counterpart and thus the Zeeman limited superconducting state cannot be reached except under special circumstances. One common way to suppress the orbital response is to fabricate a thin superconducting film and then apply the magnetic field parallel to the film surface. In the absence of SO scattering [18], this strategy can realize a purely Zeeman-mediated, first-order critical field transition [17] as long as the film thickness is much less than the coherence length. The Zeeman-limited parallel critical field $H_{c\|}$ is given by the Clogston-Chandrasekhar equation [19, 20],

$$H_{c\|}(0) = \frac{\sqrt{2}\,\Delta_0}{g\mu_{\mathrm{B}}}, \tag{1}$$

where Δ_0 is the zero temperature - zero field gap energy, μ_{B} is the Bohr magneton, and $g \sim 2$ is the Landé g-factor. We note that equation (1) is in SI units as well as all of the other equations in this report.

In contrast, if a magnetic field is applied perpendicularly to a thin superconducting film, the orbital response usually dominates, and an array of quantized vortices is induced whose areal density is proportional to the field strength. The perpendicular critical field is reached when the vortex density is sufficiently high for the vortex cores to overlap,

$$H_{c2}(0) = \frac{\Phi_0}{2\pi\xi^2}, \tag{2}$$

where Φ_0 is the flux quantum and ξ is the Pippard coherence length [16]. Equations (1) and (2) represent critical fields for $T \ll T_c$. However, the low temperature critical fields of some of the Re-Al bilayers in this study were well beyond the 9 T limit of our measuring system. Fortunately, reasonably accurate estimates of the both $H_{c\|}(0)$ and $H_{c2}(0)$ can be extracted from the temperature dependence of the respective critical fields near T_c. We use the Werthamer-Helfand-Hohenberg formula [21] to obtain the $T = 0$ orbital critical field,

$$H_{c2}(0) = -0.693\left(\frac{dH_{c2}}{dT}\right)_{T_c} \times T_c. \tag{3}$$

Similarly, the parallel critical field can be estimated via the following [5],

$$H_{c\|}^2(0) = -0.693\left(\frac{dH_{c\|}^2}{dT}\right)_{T_c} \times T_c. \tag{4}$$

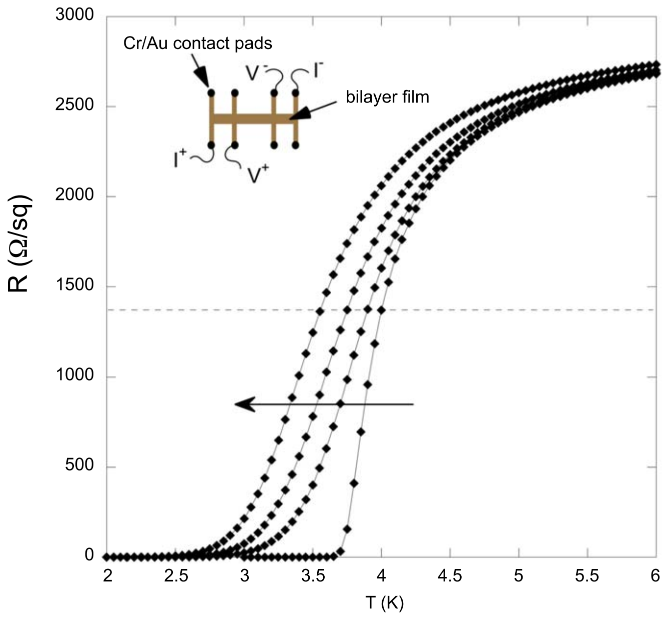

Figure 1. Sheet resistance as a function of temperature of a 3.0 nm Re film. The arrow indicates increasing magnetic field. The traces represent superconducting transitions in perpendicular magnetic fields of 0 T, 1.5 T, 3.0 T, and 5.0 T. The horizontal dashed line indicates the midpoint of the transitions. Inset: schematic of bilayer geometry and 4-wire configuration.

equation (4) accounts for both the Zeeman and orbital responses of the superconductor [5]. Of course, the orbital response of a thin film to parallel field is greatly suppressed if $d \ll \xi$, but it is not zero. In contrast, the Zeeman response is independent of field orientation but it is inhibited by SO scattering. As a consequence of these effects, the measured $H_{c\|}$ is often much larger than that of equation (1). The intrinsic SO scattering rate is proportional[18] to Z^4, where Z is the atomic number of the element Consequently, all but the lightest of the elemental superconductors (such as Al and Be) have significant SO enhancements of $H_{c\|}$.

4. Results and discussion

Shown in figure 1 are resistive transitions of a pure 3 nm Re film at several applied perpendicular magnetic fields. These resistive superconducting transitions represent the baseline critical field behavior the Re film with no Al over-layer. The transition temperature of the film $T_c = 4.0$ K was defined as the midpoint of the resistance trace, which is indicated by the horizontal dashed line in the plot. It's evident from the raw data in figure 1 that the zero temperature perpendicular critical field, $H_{c2}(0)$ of this 3 nm Re film is quite high. A 5 T perpendicular field suppresses the transition temperature by only 10%. Note that the sheet resistances of all films were well below the quantum resistance $R_Q = h/e^2$, where h is Planck's constant and e is the electron charge. This indicates that, although the films were significantly disordered, they were not near the superconductor-insulator transition [22, 23]. The transition temperatures in figure 1 are considerably higher than that of bulk Re ($T_c = 1.7$K), but it has been known since the mid 1950's that Re has a compliant T_c which can be non-perturbatively enhanced over its bulk value by pressure, strain, and/or milling [24–27].

Previously reported transmission electron micrographs of thin ($d_{\text{Re}} < 6$ nm) quench-condensed Re films reveal a highly disordered base interspersed with ∼2 nm crystallites [5]. The degree to which the Al over-layer modifies the underlying Re structure is unknown. In general, disorder can increase H_{c2} via two mechanisms. The first, and most obvious, is that disorder reduces the mean-free-path in the normal state and, correspondingly, the coherence length in the superconducting phase. Shorter coherence lengths result in high critical fields as per equation (2). The second mechanism is mediated via vortex pinning. In the presence of strong pinning the Abrikosov vortex array cannot readily move into the film, which inhibits the collapse of the superconducting phase [16]. However, strong pinning is usually associated with non-equilibrium dynamics such as hysteresis, slow non-exponential relaxations, and avalanches. Indeed, in limit of very strong pinning the classic M-H hysteresis loop of a type-2 superconductor can be profoundly modified by series of thermo-magnetic vortex avalanche events [28]. We do not believe that vortex pinning plays a significant role in either the critical field behavior of pure Re films or their Re/Al counterparts. Low temperature R-H isotherms simply do not exhibit an appreciable hysteresis. Nor do we observe avalanche-type events in the magnetic field traces.

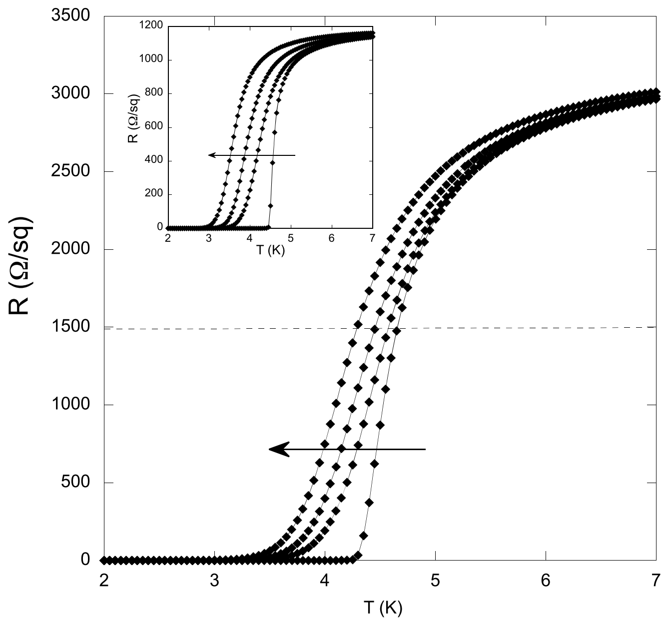

Figure 2. Sheet resistance as a function of temperature of a 3.0/1.5 nm Re/Al bilayer. The arrows indicate increasing perpendicular magnetic field. The traces represent superconducting transitions in magnetic fields of 0 T, 1.5 T, 3.0 T, and 5.0 T. Inset: corresponding data for a 3.0/2.5 nm Re/Al bilayer.

Now we turn to the bilayer critical field behavior. Shown in figure 2, is the temperature dependence of the sheet resistance of a 3/1.5 nm and a 3/2.5 nm Re/Al bilayer. This data is to be compared with that of the 3 nm Re film of figure 1. Note that the $H = 0$ transition temperature of these two bilayers is significantly higher than that of the 3 nm Re film. Aluminum films have a variable T_c, but films of thickness less than 5 nm typically [29, 30] have $T_c = 2 - 3$ K, which is considerably lower than that of the Re layer. Assuming that the two components of the bilayer interact via the classic proximity effect[1, 2], one would expect the Re/Al bilayers to have 2 K $< T_c <$ 4 K. We believe that the anomalously high T_c of the bilayers in figure 2, i.e. $T_c > 4$ K, may be a consequence of disorder, as we discuss below.

The T_c of thin, critically disordered rhenium films is suppressed with increasing sheet resistance. Indeed, Re films undergo a phase-mediated superconductor-insulator transition [22, 31] at a sheet resistance near the quantum resistance $R_Q = h/e^2$. As the film resistance increases with decreasing thickness and/or oxidation the phase stiffness of the superconducting order parameter is diminished. This leads to monotonic decrease in T_c. Shown in figure 3 are the transition temperatures of 3 Re films as a function of their sheet resistance. The black diamond and the open square refer to a 2.5nm and a 2.0 nm Re film, respectively. The transition temperature of these two films was measured immediately after deposition. The black squares represent a 1.7 nm film that was sequentially exposed to atmosphere for 10 minute intervals in order to induce oxidation. The transition temperature was measured after each exposure. Note that T_c decreases approximately linearly with increasing sheet resistance. Furthermore, T_c extrapolates to zero at $R = 0.9R_Q$. The quasi-linear suppression of T_c is consistent with similar behavior observed in thin amorphously disordered films of W-Re [32] and Mo-Ge [33]. Renormalization group analysis accounting for electron-electron interactions also predicts a quasi-linear suppression of T_c for sheet resistances $R \ll R_Q$ [34]. At higher sheet resistances the superconducting phase is suppressed and the films exhibit insulating behavior, as can be seen in figure 4. So, in principle, the addition of an Al over-layer on a thin Re film can have countervailing effects. On one hand, if $T_c^{\text{Al}} < T_c^{\text{Re}}$, then the bilayer T_c will lie below T_c^{Re} by virtue of the proximity effect[1]. On the other hand, the Al layer increases the electronic thickness of the system thereby possibly reducing $e - e$ interactions and increasing T_c^{Re} as per the data in figure 3. Thus the bilayer T_c is not necessarily a monotonic function of the Al thickness.

In figure 5 we plot H_{c2} as a function of temperature near T_c for a 3 nm Re film, as well as the 3/1.5 nm, 3/2.5 nm, and 3/3.0 nm Re/Al bilayers. Note that the perpendicular critical field of all the samples increases linearly with decreasing temperature. The solid lines are a linear least-squares fit to the data, and their slopes, as indicated in the plot, provide an indirect measure of $H_{c2}(0)$ via equation (3). Neglecting the Zeeman response, we estimate that $H_{c2}(0) \approx 30$ T for the Re film and $H_{c2}(0) \approx$ 45, 16, 8 T for the 3/1.5, 3/2.5, and 3/3.0 bilayers, respectively. These upper critical fields are extremely high for elemental systems. For comparison, in the inset of figure 5 we present $H_{c2}(T)$ near T_c for a 4 nm Al film capped with 0.3 nm of Au. The Au served to induce some

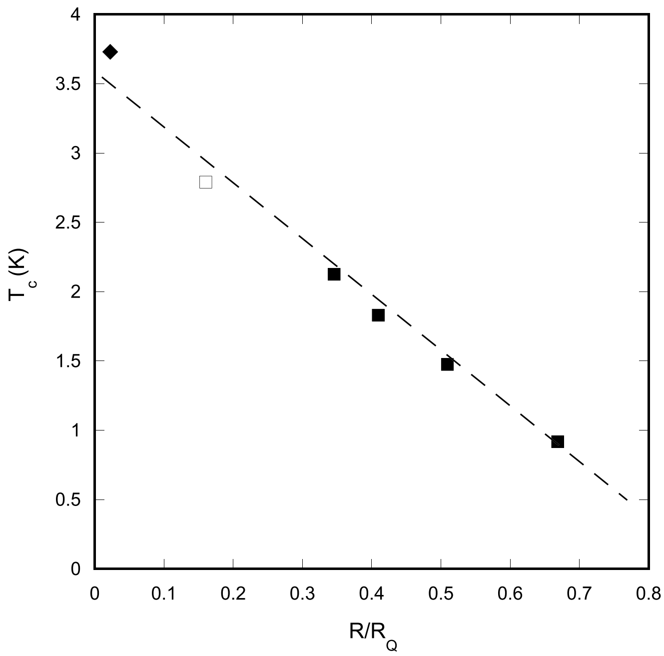

Figure 3. Re film superconductor-insulator transition. The transition temperature of several Re films is plotted as a function their normalized sheet resistance. The diamond and open square symbols refer to a 2.5 nm and a 2.0 nm Re film, respectively. Both of these were measured immediately after deposition. The black squares refer to a 1.7 nm thick Re film that was repeatedly exposed to atmosphere and remeasured after each exposure. The dashed line is provided as a guide to the eye.

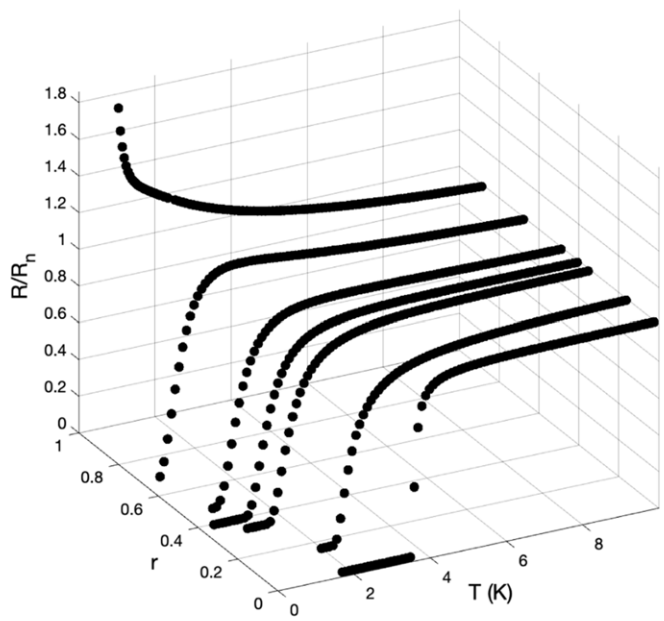

Figure 4. Zero field superconductor-insulator transition for the Re films in figure 4. R_n is the normal state sheet resistance and $r = R_n/R_Q$.

spin-orbit scattering in the Al in order to quench the Zeeman response. We note that the estimated critical field of the Al film $H_{c2}(0) \approx 0.24$ T is a factor of 60 lower than that of 3/1.5 nm bilayer, although the Al film and that bilayer are of comparable total thickness.

We have also made direct low temperature measurements of H_{c2} for a 2.5 nm Re film. These data were taken at temperatures $T << T_c$ in order to verify the accuracy of the extrapolations based on equation (3). Shown in figure 6 are a series of critical field transitions of a 2.5 nm Re capped with 1.0 nm of Ge to prevent oxidation. Germanium capped Re films have a reasonable shelf life of several days. The data in figure 6 were obtained at the National High Magnetic Field Laboratory in Tallahassee, FL. The plot shows the critical field behavior of the film

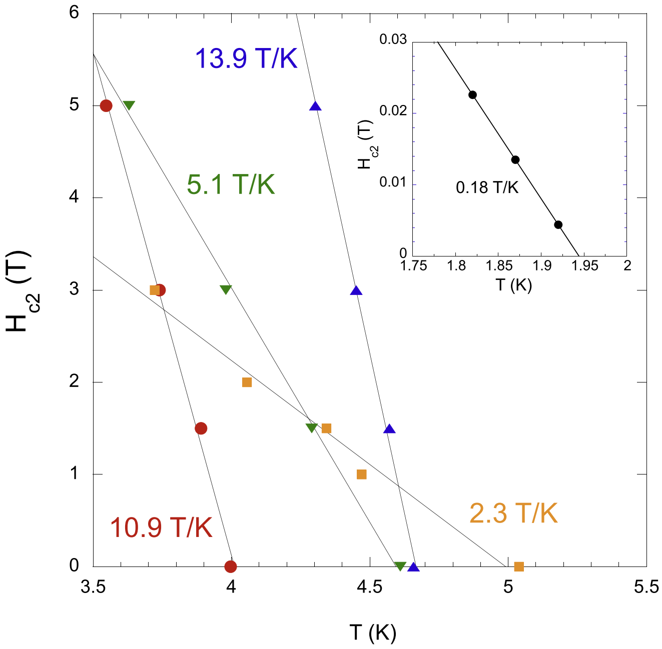

Figure 5. Temperature dependence of the perpendicular critical field of a 3 nm Re film (red circles), along with that of a 3/1.5 nm (blue triangles), 3/2.5 nm (green triangles), and 3/3.0 nm (orange squares) Re/Al bilayers. The lines represent a linear least-squares fit to the data with the indicated slopes. Inset: Temperature dependence of the perpendicular critical field of a 4 nm Al film capped with 0.3 nm Au.

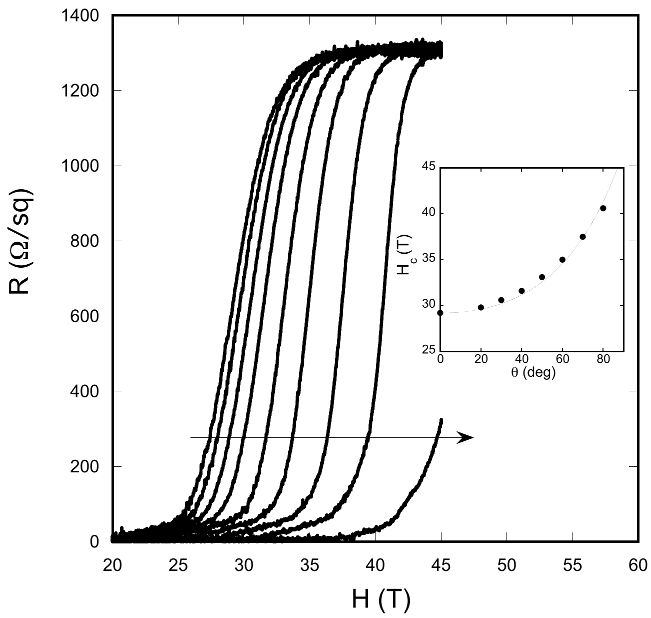

Figure 6. Critical field transitions of a 2.5 nm Re film capped with 1 nm of Ge at several different tilt angles between the normal to the bilayer surface and the applied field. From left to right, the data traces correspond to tilt angles $\theta = -1°$, 19°, 29°, 39°, 49°, 59°, 69°, 79°, where $\theta = 0$ corresponds to perpendicularly applied field. These data were taken at 0.38 K and the maximum field of the solenoid was 45 T. Inset: Midpoint critical field as a function of angle. The line represents the prediction of equation (5).

as a function of field orientation relative to the film surface normal, where $\theta = 0°$ corresponds to perpendicular orientation and $\theta = 90°$ corresponds to field oriented parallel to the film surface. For this particular sample $T_c = 4$ K and the data were taken at $T = 0.38$ K. As expected, the critical field rises rapidly as one approaches $\theta = 90°$. Note that the parallel critical field of this sample was beyond the 45 T upper limit of the solenoid. Nevertheless, our primary interest is in the perpendicular critical field, which is easily read directly from the plot. The $\theta = 0$ midpoint critical field is $H_{c2} \approx 30.2$ T. This is in excellent agreement with our estimation of $H_{c2}(0)$ for the 3 nm Re film in figure 6.

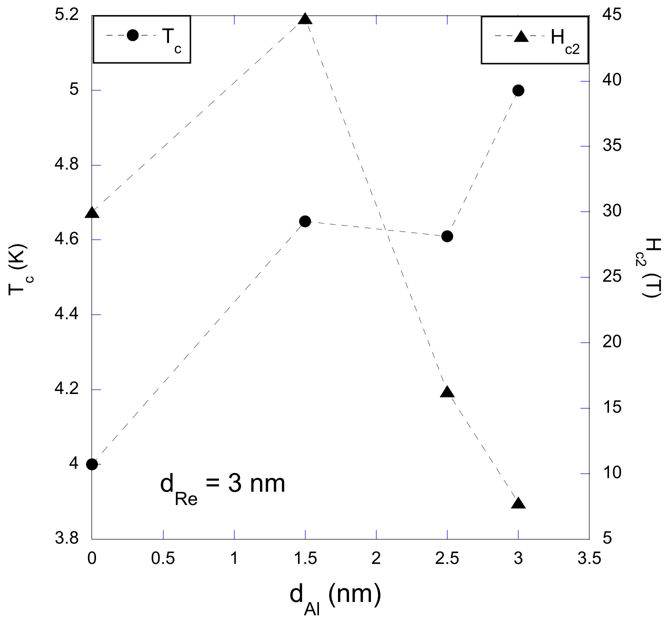

Figure 7. Transition temperature and critical field of bilayers plotted as a function of Al thickness. All of the samples had a Re thickness of 3 nm.

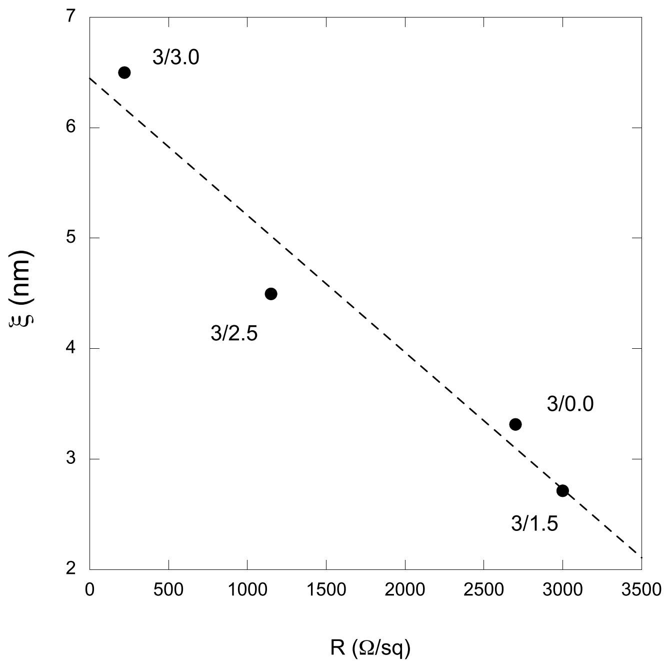

Figure 8. Coherence length as function of normal state sheet resistance. The corresponding Re/Al thickness for each data point is shown. The dashed line is provided as a guide to the eye.

The inset in figure 6 shows the angular dependence of the low temperature critical field of the 2.5 nm Re film. The solid line is a least squares fit to the Tinkham formula for a two-dimensional superconductor [16],

$$\frac{H_c(\theta)\cos\theta}{H_{c2}} + \left(\frac{H_c(\theta)\sin\theta}{H_{c\|}}\right)^2 = 1 \quad (5)$$

where $H_{c\|}$ was varied for the best fit. The angular dependence of the critical field agrees well equation (5) with $H_{c\|} = 46$ T.

In figure 7 we present a synopsis of the transition temperatures and critical fields of the bilayers used in this study. As we mentioned earlier, all of the bilayers had a Re thickness of 3 nm but varied in Al layer thickness, which is plotted on the x-axis. Note that the Al layers in this range of thicknesses produces a significant enhancement of T_c over the bare Re value. As discussed earlier, this effect cannot be explained by the proximity effect but is probably a consequence of the fact that the sheet resistance of the bilayer decreases with increasing Al thickness. The $d_{\mathrm{Al}} = 3.0$ nm bilayer has a total thickness of 6 nm, $T_c = 5$ K, and a normal state sheet resistance $R_n = 220\Omega$. In comparison, a 6 nm thick Re film has a comparable $T_c \approx 4.8$ K and a sheet resistance of $R_n = 600\Omega$. Finally, we point out the very large enhancement of the critical field for $d_{\mathrm{Al}} = 1.5$ nm, H_{c2}. This bilayer has a critical field that is roughly 50% larger than that of the underlying Re layer. The coherence lengths of the bilayers, as determined from equation (2), are shown in figure 8.

5. Summary

In summary, we find that the critical field of a thin Al film can be greatly enhanced by depositing in on similarly thick Re film. For example a 3 nm Al film deposited on a 3 nm Re has a perpendicular critical field that is approximately 30 times greater than that of a standalone Al film. Furthermore in the thickness range of this study the bilayers have a higher transition temperature than either of their standalone components. There continues to be a substantial interest in liquid-helium temperature superconductors that can be used in quantum information and computation technologies [10, 11, 35]. We conclusively demonstrate that Al deposited on a thin Re layer substantially improves both the magnetic field tolerance of the Al layer and its transition temperature without compromising the desirable metallurgical characteristics of the Al. Extending the present studies to direct ultra-high field measurements of the low-temperature magnetotransport and tunneling density of states properties of the Al component of the bilayers should prove enlightening.

Acknowledgments

The magneto-transport measurements were performed by P.W.A. A.M.O. and F.N.W with the support of the U.S. Department of Energy, Office of Science, Basic Energy Sciences, under Award No. DE-FG02-07ER46420. High Field measurements were carried out at the National High Magnetic Field Laboratory by S.K.K. and D.G. The NHMFL is supported by the National Science Foundation through NSF/DMR-1644779 and the State of Florida. S.K.K. acknowledges the support from the National Science Foundation through Excellence in Research program under Award No. DMR-2302420.

Data availability statement

All data that support the findings of this study are included within the article (and any supplementary files).

ORCID iDs

F N Womack https://orcid.org/0009-0008-1039-1507
Á M Ortega https://orcid.org/0009-0000-1136-6970
P W Adams https://orcid.org/0000-0002-8412-0303

References

[1] de Gennes P G 1964 *Rev. Mod. Phys.* **3** 225
[2] Deutscher G and de Gennes P G 1969 *Superconductivity* ed E D Parks (Marcel Dekker)
[3] Hauser J J and Theuerer H C 1965 *Phys. Letters* **1** 270
[4] Kouh T and Valles J M Jr. 2003 *Phys. Rev.* B **6** 140506(R)
[5] Womack F N, Young D P, Browne D A, Catelani G, Jiang J, Meletis E I and Adams P W 2021 *Phys. Rev.* B **1** 024504
[6] Teknowijoyo S and Gulian A 2024 *Supercond. Sci. Technol.* **3** 035005
[7] Pettit R B and Silcox J 1976 *Phys. Rev.* B **1** 2865
[8] Chubov P N, Eremenko V V and Pilipenko Y A 1969 *Sov. Phys. JETP* **2** 389
[9] van Weerdenburg W M J, Kamlapure A, Fyhn E H, Huang X, van Mullekom N P E, Steinbrecher M, Krogstrup P, Linder J and Khajetoorians A A 2023 *Sci. Adv.* **9** eadf5500
[10] Hazard T M, Gyenis A, Di Paolo A, Asfaw A T, Lyon S A, Blais A and Houck A A 2019 *Phys. Rev. Lett.* **1** 010504
[11] Grnhaupt L *et al* 2019 *Nat. Mater.* **1** 816
[12] Kjaergaard M, Schwartz M E, Braumüller J, Krantz P, Wang J I-J, Gustavsson S and Oliver W D 2020 *Annu. Rev. Condens. Matter Phys.* **11** 369
[13] Borisov K *et al* 2020 *Appl. Phys. Lett.* **1** 120502

[14] Shabani J *et al* 2016 *Phys. Rev.* B **9** 155402
[15] Zhao L, Iftikhar Z, Larson T F Q, Arnault E G, Watanabe K, Taniguchi T, Amet F and Finkelstein G 2023 *Phys. Rev. Lett.* **1** 176604
[16] Tinkham M 1996 *Introduction to Superconductivity* (McGraw-Hill)
[17] Fulde P 1973 *Adv. Phys* **22** 667
[18] Meservey R and Tedrow P M 1978 *Phys. Rev. Lett.* **41** 805
[19] Clogston A M 1962 *Phys. Rev. Lett.* **9** 266–7
[20] Chandrasekhar B S 1962 *Appl. Phys. Lett.* **1** 7–8
[21] Werthamer N R, Helfand E and Hohenberg P C 1966 *Phys. Rev.* **147** 295
[22] Sacepe B, Feigel'man M and Klapwijk T M 2020 *Nat. Phys.* **16** 734
[23] Dobrosavljevic V, Trivedi N and Valles, Jr J M 2012 *Conductor Insulator Quantum Phase Transitions* (Cambridge University Press)
[24] Hulm J K and Goodmann B B 1957 *Phys. Rev.* **106** 659
[25] Mito M *et al* 2016 *Sci. Rep.* **6** 36337
[26] Pappas D P *et al* 2018 *Appl. Phys. Lett.* **112** 182601
[27] Song C, Heitmann T W, DeFeo M P, Yu K, McDermott R, Neeley M, Martinis J M and Plourde B L T 2009 *Phys. Rev.* B **79** 174512 When Re film are deposited onto 850 °C substrates one obtains the bulk T_c, see
[28] Young D P, Moldovan M, Adams P W and Prozorov R 2005 *Supercond. Sci. Technol.* **18** 1
[29] Tedrow P M and Meservey R 1982 *Phys. Rev.* B **25** 171
[30] Wu W and Adams P W 1994 *Phys. Rev. Lett.* **7** 1412
[31] Butko V Y and Adams P W 2001 *Nature* **409** 161
[32] Raggy H R, Laibowitz R B, Chaudhari P and Maekawa S 1983 *Phys. Rev.* B **28** 6607
[33] Graybeal J M and Beasley M R 1984 *Phys. Rev.* B **29** 4167
[34] Finkel'stein A M 1987 *JETP Lett.* **45** 46
[35] Niepce D, Burnett J and Bylander J 2019 *Phys. Rev. Applied* **11** 044014